

Abundance ratios in hierarchical galaxy formation

D. Thomas

Universitäts-Sternwarte München, Scheinerstr. 1, D-81679 München, Germany

12 September 2018

ABSTRACT

The chemical enrichment and stellar abundance ratios of galaxies which form in a hierarchical clustering scheme are calculated. For this purpose I adopt the star formation histories (SFH) as they are delivered by semi-analytic models in Kauffmann (1996). It turns out that the average SFH of cluster ellipticals does not yield globally α -enhanced stellar populations. The star burst that occurs when the elliptical forms in the major merger plays therefore a crucial role in producing α -enhancement. Only under the assumption that the IMF is significantly flattened with respect to the Salpeter value during the burst, a Mg/Fe overabundant population can be obtained. In particular for the interpretations of radial gradients in metallicity and α -enhancement, the mixing of global and burst populations are of great importance. The model predicts bright field galaxies to be less α -enhanced than their counterparts in clusters.

Key words: stars: luminosity function, mass function – galaxies: elliptical and lenticular, cD – galaxies: abundances – galaxies: formation – galaxies: evolution – cosmology: theory

1 INTRODUCTION

Simulations of hierarchical galaxy formation in a CDM universe (Kauffmann, White & Guiderdoni 1993; Cole et al. 1994) are based on semi-analytic models in the framework of Press-Schechter theory. They aim to describe the formation of galaxies in a cosmological context, and therefore are designed to match a number of constraints like B and K luminosity functions, the Tully-Fisher relation, redshift distribution, and slope and scatter of the colour-magnitude relation (CMR). Since in a bottom-up scenario more massive objects form later, and are therefore younger and bluer – in contrast to the observed CMR – the original works were substantially suffering from the problem of creating luminous red elliptical galaxies (Kauffmann et al. 1993; Lacey et al. 1993; Cole et al. 1994). It is also not a priori clear if these models which yield strong evolution at intermediate redshift (Kauffmann, Charlot & White 1996) would be able to reproduce the small scatter of the CMR and the Mg- σ relation. On the other hand, these constraints can be easily explained by the classical single burst picture for elliptical galaxy formation, assuming passive evolution after a short formation epoch at high redshift, provided that subsequent stellar merging is negligible (Bower, Kodama & Terlevich 1998). However, the more recent models by Kauffmann (1996, hereafter K96) and Baugh, Cole & Frenk (1996) reproduce the above relations with a scatter which is in remarkably good agreement with observational data (Bower, Lucey & Ellis 1992; Bender, Burstein & Faber 1993; Jørgensen, Franx & Kjørgaard 1996). The correct slope of the CMR can be obtained in a hierarchi-

cal scheme, if metal enrichment and metallicity-dependent population synthesis models are taken into account (Kauffmann & Charlot 1998; Cole et al., in preparation). In such models, the slope of the CMR is only driven by metallicity, as in the classical models by Arimoto & Yoshii (1987). Note however, that in the framework of the inverse wind models (Matteucci 1994) the CMR slope could be in principle produced from a combination of both age and metallicity, since in these models more massive galaxies are assumed to be older.

In this paper I aim to discuss how far hierarchical formation models are able to accomplish a further important constraint, namely the formation of α -enhanced stellar populations hosted by luminous ellipticals (Peletier 1989; Worthey, Faber & González 1992; Davies, Sadler & Peletier 1993). Models of chemical evolution show that this constraint can be matched by the single collapse model being characterised by short star formation time-scales of the order $10^8 - 10^9$ yr (e.g. Matteucci 1994; Thomas, Greggio & Bender 1999; Jimenez et al. 1999), and it has been questioned by Bender (1997) whether the observed [Mg/Fe] overabundance is compatible with hierarchical models. However, abundance ratios and the enrichment of α -elements have not been investigated so far in hierarchical models. For this purpose, I consider typical star formation histories provided by semi-analytic models for hierarchical galaxy formation (K96) and explore the resulting abundance ratios of magnesium and iron.

The paper is organised as follows. In Section 2 the model

arXiv:astro-ph/9901226v1 18 Jan 1999

of chemical enrichment is briefly described. Average and bursty star formation histories are then analysed in Sections 3, 4 and 5. The results are discussed and summarised in Sections 6 and 7.

2 THE MODEL

The idea is to follow the chemical evolution of the galaxy describing the global chemical properties of the final object and its progenitors as a whole during the merging history. In the hierarchical clustering scheme, structures are subsequently build up starting from small disc-like objects. An elliptical is formed when two disc galaxies of comparable mass merge, which is called the ‘major merger’. Before this event many ‘minor mergers’ between a central galaxy and its satellite systems happen. It is important to emphasise, that the bulk of stars, namely 70–90 per cent, forms at modest rates in the progenitor disc-galaxies *before* this ‘major merger’ event. In the star burst ignited by the latter, up to 30 per cent of the total stellar mass of the elliptical is created. In K96 many Monte Carlo simulations are performed each corresponding to one individual (final) galaxy. The SFH which is specified in K96 and adopted for the present analysis is an *average* about all these realizations.

2.1 Star formation rates

The SFH is characterised by the age distribution of the stellar populations weighted in the V -band light. In other words, the fractional contributions L_V^{SP} by stellar populations to the total V -light as a function of their ages t are specified. Equation 1 shows how this translates into a star formation *rate* ψ :

$$L_V^{\text{SP}}(t_0, t_1) = \frac{\int_{t_0}^{t_1} \psi(t) L_V^{\text{SSP}}(t) dt}{\int_0^{t_{\text{univ}}} \psi(t) L_V^{\text{SSP}}(t) dt}. \quad (1)$$

Here, the interval $[t_0, t_1]$ denotes the age bin of the population, t_{univ} is the assumed age of the universe, i.e. $t_{\text{univ}} \approx 13$ Gyr for the cosmology adopted in K96 ($\Omega_m = 1$, $\Omega_\Lambda = 0$, $h = 0.5$). The V -light of a simple stellar population $L_V^{\text{SSP}}(t)$ as a function of its age and metallicity is taken from Worthey (1994). In this paper, the star formation rate ψ as a function of time is chosen such that a set of stellar populations of various ages and metallicities is constructed which exactly covers the age distribution of the K96 models.

2.2 Chemical enrichment

The chemical evolution is calculated by solving the usual set of differential equations (e.g. Tinsley 1980). The enrichment process of the elements hydrogen, magnesium, iron, and total metallicity is computed, no instantaneous recycling is assumed. In particular, the delayed enrichment by Type Ia supernovae is taken into account following the model by Greggio & Renzini (1983). The inclusion of Type Ia is crucial for interpreting Mg/Fe ratios, since SNe Ia substantially contribute to the enrichment of iron. The evolution code is calibrated on the chemical evolution in the solar neighbourhood (Thomas, Greggio & Bender 1998). The ratio of SNe Ia to SNe II is chosen such that observational

constraints like supernova rates, the age-metallicity relation and the trend of Mg/Fe as a function of Fe/H in the solar neighbourhood are reproduced. The SN II nucleosynthesis prescription is adopted from Thielemann, Nomoto & Hashimoto (1996) and Nomoto et al. (1997), because the stellar yields from Woosley & Weaver (1995) are unable to account for the [Mg/Fe] overabundance in the solar neighbourhood (Thomas et al. 1998).

The IMF is truncated at $0.1 M_\odot$ and $40 M_\odot$. The slope above $1 M_\odot$ is treated as a parameter, below this threshold a flattening according to recent HST measurements (Gould, Bahcall & Flynn 1997) is assumed. This flattening at the low-mass end does not significantly affect α/Fe ratios. It should be noted that stars more massive than $40 M_\odot$ are expected to play a minor role in the enrichment process, because of their small number and the fall-back effect (Woosley & Weaver 1995). Moreover, the mean [Mg/Fe] overabundance in the metal-poor halo stars of our Galaxy is well reproduced for an IMF with the above truncation and Salpeter slope $x = 1.35$ (Salpeter 1955), if Thielemann et al. nucleosynthesis is adopted (Thomas et al. 1998). The V -luminosity averaged abundances in the stars are computed by using SSP models from Worthey (1994). For details I refer the reader to Thomas et al. (1998, 1999).

Finally, two simplifications of the present model should be mentioned:

(i) A one-phase interstellar medium (ISM) is assumed. Kauffmann & Charlot (1998), instead, distinguish between cold and hot gas allowing mass transfer among these two components. Since stars form out of cold gas, this process basically controls the feed-back mechanism of star formation. The resulting effects on the star formation rate, however, are already covered, since I directly adopt the SFH from K96. The influence on the abundance *ratio* of Mg and Fe is expected to be negligible, as long as these elements do not mix on significantly different time-scales.

(ii) The final galaxy is treated as the whole single-unit from the beginning of its evolution, the economics of the individual progenitors are not followed separately as in K96. Hence, the simulations do not directly include galactic mass loss taking place during disc galaxy evolution (K96) as well as mass transfer between the progenitor systems. The fraction of gas converted to stars is adjusted to global metallicities typically observed in the respective galaxy type. The impact on the *global* properties of the *final* galaxy, however, is expected to be small. In particular, abundance *ratios* of non-primordial elements like Mg and Fe are not significantly affected by mass loss and gas transfer, unless one allows for selective mechanisms. However, in the framework of the present analysis, this option shall only be discussed in a qualitative fashion.

3 GLOBAL POPULATIONS

Figs. 1 and 2 show the global average SFHs as they are constrained for cluster elliptical and spiral galaxies in the K96 model. The lower x-axis denote ages (look-back time), the evolutionary direction of time therefore goes from the right to the left. The evolution with redshift for an $\Omega_m = 1$, $\Omega_\Lambda = 0$ cosmology (adopted in K96) is given by the upper

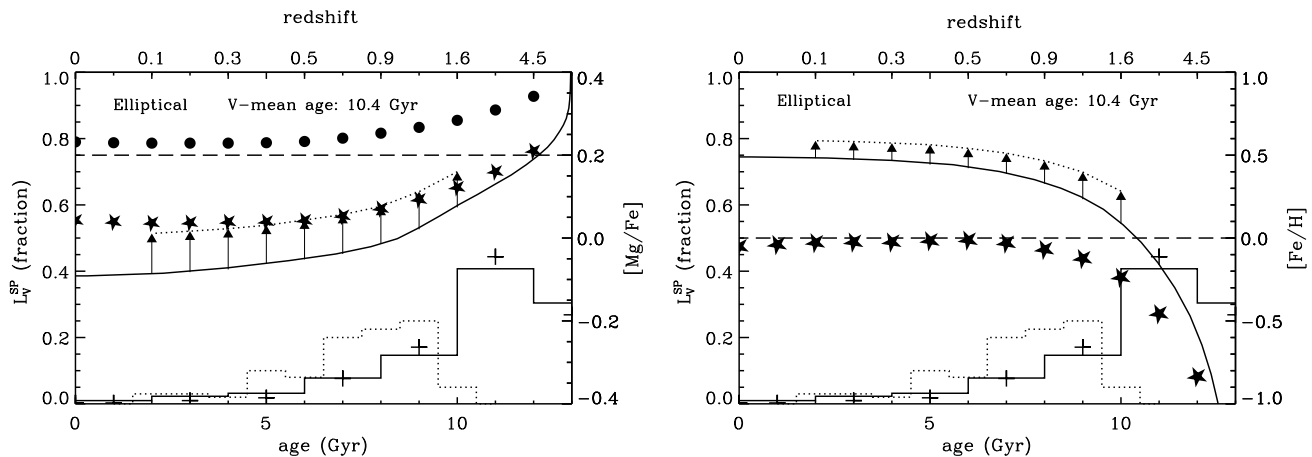


Figure 1. The star formation history of an average cluster elliptical. The lower and upper x-axis specify age (look-back time) and redshift ($\Omega_m = 1, \Omega_\Lambda = 0$), respectively. The left y-axis denote a ‘fraction’. The histogram shows the fractional contribution to the total light in the V -band from each stellar population of a specific age (see eqn. 1). The plus-signs denote the respective contribution to the total mass of the object. The scales for the underlying abundance ratios Mg/Fe (left-hand panel) and Fe/H (right-hand panel) are given by the right-hand y-axis: interstellar medium abundance (solid line), V -average in the composite stellar population (star symbols), the V -average in the composite stellar population for a flat IMF ($x = 0.8$, filled circles). The dotted histogram indicates the fractional number distribution of the major merger epochs of elliptical formation as they come out in the individual Monte Carlo realizations (K96). The arrows to the dotted line at the various merger epochs give the stellar abundance ratios of the newly created burst population formed in the major merger (see text). The horizontal dashed lines mark the observational constraints for α -enhancement and metallicity of elliptical galaxies, respectively.

x-axis. The histogram shows the quantity $L_V^{\text{SP}}(t_0, t_1)$ as it is explained in Section 2. In the elliptical case (Fig. 1), more than 70 per cent of the light in the V -band comes from stars which have formed in the first 3 Gyr at redshift $z \gtrsim 2$. The SFH of the spiral (Fig. 2), instead, is much more extended towards lower redshift. With a V -mean age of 6.2 Gyr, the latter thus leads to significantly younger populations than the SFH of the average elliptical (10.4 Gyr). The plus signs in Figs. 1 and 2 denote the fractional contributions from the various populations to the total mass of the object. Owing to their stellar remnants, old populations contribute more to the total mass than to the light of the object. As a consequence, in the optical band the weight of young (old) populations is larger (smaller) with respect to their actual mass. This pattern is particularly prominent in the young and old spiral populations.

The abundance ratios of Mg/Fe (left-hand panels) and Fe/H (right-hand panels) as they result from the chemical evolution model are shown with the scale on the right y-axis, respectively. The chemical evolution of the ISM is denoted by the solid line, the filled star symbols show the V -luminosity weighted average abundance ratios of the respective composite stellar population of the galaxy as a function of age (hence formation redshift). The filled circles in the left-hand panel of Fig. 1 represent the stellar mean Mg/Fe ratio if a global flattening of the IMF with $x = 0.8$ is assumed. Otherwise, Salpeter slope above $1 M_\odot$ ($x = 1.35$) is chosen.

In general, the mean abundances in the stellar populations differ from those in the ISM. Metallicity (Fe/H) is always higher, and Mg/Fe always lower in the ISM than in the V -average of the stars, because the stars archive the abundance patterns of early epochs. Since, in the case of the elliptical, star formation is much more skewed towards early

times, this discrepancy is more significant in such objects. The gas fraction which is ejected from the galaxy is chosen such that the *global* stellar populations of the elliptical have solar metallicity at low redshift (Fig. 1). This leads to an ejection of roughly 30 per cent of the baryonic mass of the galaxy during its evolution. In the case of the spiral (Milky Way), instead, 55 per cent of the gas are assumed to be ejected in order to yield solar metallicity in the ISM after 9 Gyr, roughly when the Sun was born (Fig. 2).

As a consequence, the metallicity of the ISM and the stars is higher in the elliptical than in the spiral. The Mg/Fe ratios, instead, depend mainly on the shape of the star formation rate as a function of time. Since there is no significant star formation at late times in the elliptical, $N_{\text{SNI I}}/N_{\text{SNI a}}$ is 20 times lower than in the spiral galaxy, which leads to a lower Mg/Fe in the ISM by roughly 0.1 dex. The stars, instead, store the chemical abundances of the early epochs, $\langle [\text{Mg}/\text{Fe}] \rangle_V$ is 0.04 dex higher in the elliptical galaxy than in the spiral, which is in accordance with its older mean age. Still, the stellar populations in both galaxy types exhibit roughly solar Mg/Fe ratios at low redshift, in particular $\langle [\text{Mg}/\text{Fe}] \rangle_V \approx 0.04$ dex for the elliptical. In spite of the negligible contribution of the late star formation to the mean age of the galaxy, the mean $[\text{Mg}/\text{Fe}]$ ratio is driven significantly below 0.2 dex (Fig. 1). This result clearly stands in disagreement to the observational indications that (bright) elliptical galaxies host stellar populations which are α -enhanced by at least 0.2 – 0.3 dex (Peletier 1989; Worthey et al. 1992; Davies et al. 1993).

Fig. 1 demonstrates that with Salpeter IMF a super-solar Mg/Fe ratio is only obtained at the very early stages of the evolution, namely in the first Gyr. A star formation mode which is more skewed towards these early formation ages would lead to older ages and a higher de-

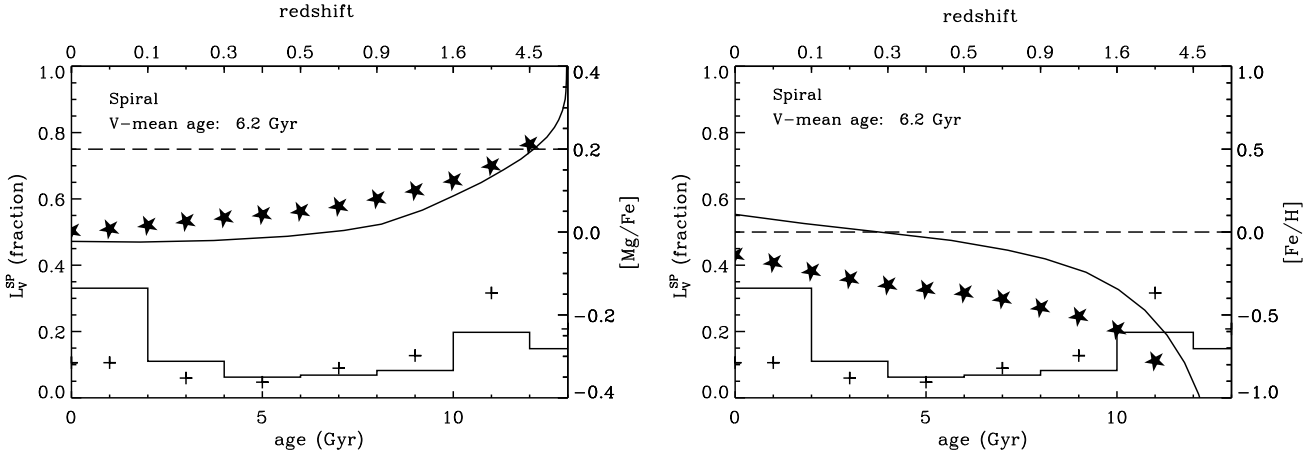


Figure 2. The star formation history of an average spiral. Axis and symbols are explained in Fig. 1.

gree of α -enhancement. One may argue that the average SFH considered here does not apply to *bright* ellipticals in which the observed α -enhancement is most significant. However, in the K96 simulations brighter objects are on average younger (Kauffmann & Charlot 1998), and do not experience SFHs that are more skewed towards high redshift than the present example. They are therefore unlikely to exhibit higher Mg/Fe ratios than calculated here.

The star formation time-scales that are required to obtain $[\alpha/\text{Fe}] \approx 0.2$ for different IMF slopes are discussed in Thomas et al. (1999). The filled circles in the upper-left panel of Fig. 1 demonstrate that the shallower IMF with $x = 0.8$ can reconcile the extended SFH with α -enhancement. However, particularly in the hierarchical picture in which the formation of different galaxy types can be traced back to the same (or similar) building blocks at early epochs, a flattening of the IMF restricted to elliptical galaxies does not seem to provide a compelling solution.

From Fig. 1 one can also understand that only galaxy formation scenarios in which star formation *terminates* after 1–2 Gyr lead to $\langle [\text{Mg}/\text{Fe}] \rangle_V \gtrsim 0.2$ dex. The classical monolithic collapse provides such a star formation mode. In the hierarchical scheme, instead, (low) star formation at later stages is unavoidable, which directly leads to lower Mg/Fe ratios in the stars that form out of the highly SNIa enriched ISM at lower redshift.

4 BURST POPULATIONS

The SFHs considered here apply to the *global* properties of the galaxy populations. However, in the picture of hierarchical clustering star bursts that are induced by mergers play an important role for the interpretation of (particularly central) abundance features. The star burst during the major merger forms 10–30 per cent of the final stellar mass, which is likely to dominate the galaxy core, since the gas is driven to the central regions of the merger remnant (Barnes & Hernquist 1996). In this section I shall investigate the abundance patterns of the population that results from a 0.1 Gyr star burst triggered by the major merger which forms the final elliptical.

4.1 Universal IMF

In Fig. 1 the dotted histogram denotes the distribution of these major merger events among the elliptical galaxy population. At the given epoch when the star burst occurs, the new stellar population forms out of the ISM whose abundances are shown by the solid line in Fig. 1. Owing to the short duration of the star burst, the mean Mg/Fe ratios in the newly created stars are higher than the initial values in the ISM as indicated by the arrows and the dotted line (left-hand panel of Fig. 1). The slope of the IMF is assumed Salpeter also during the burst. It turns out that, due to the extremely low Mg/Fe ratios and the high metallicities in the ISM at the merger epoch, such star bursts are inappropriate to raise Mg/Fe up to a level consistent with observational values. The resulting Mg/Fe does not differ from the mean average in the global stellar populations.

The metallicity Fe/H, instead, increases to even higher values between 0.3 and 0.5 dex, depending on the burst epoch (upper-right panel of Fig. 1). Under the assumption that the entire central population forms in the major burst the model leads to radial metallicity gradients of 0.3–0.5 dex from the inner to the outer parts of the galaxy, in contradiction to observational measurements of ~ 0.2 dex per decade (Davies et al. 1993; Kuntschner 1998). A mixture of 3/4–1/3 between burst and global population in the galaxy nucleus is required to smooth the gradient down to the observed value.

The results shown in Fig. 1 unfold the principle dilemma of the hierarchical picture: the initial conditions in the ISM at the burst epoch, namely super-solar metallicity and sub-solar Mg/Fe, are highly unfavourable in producing α -enhanced populations. As shown in Thomas et al. (1999), this incapability of late merger events is independent of the burst time-scale and SN Ia rates during the burst. The most promising way out to reconcile an intermediate or late merger with α -enhancement is to assume a flattening of the IMF during the star burst.

4.2 Variable IMF

The arrows and dotted lines in Fig. 3 show the abundance patterns (left-hand panel: Mg/Fe, right-hand panel: Fe/H)

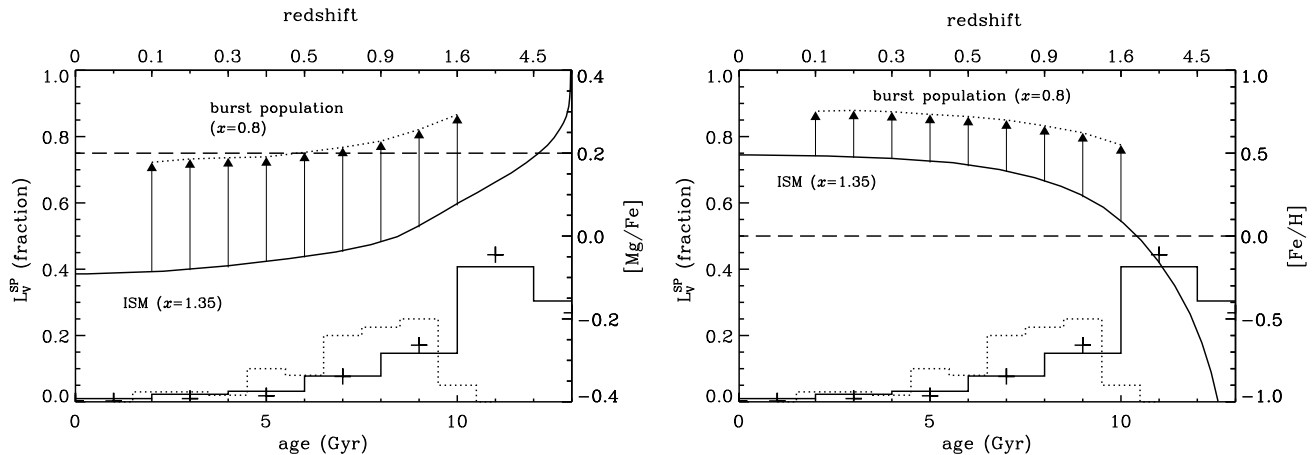


Figure 3. Abundance ratios for the average cluster elliptical. Axis and symbols are explained in Fig. 1. A flattening of the IMF ($x = 0.8$) during the major merger burst is assumed. For the evolution of the global interstellar medium (solid line), instead, Salpeter IMF ($x = 1.35$) is adopted.

Table 1. The average abundance ratios for different mixtures in V -light of the global (IMF slope $x = 1.35$) and burst ($x = 0.8$) populations. $[\text{Fe}/\text{H}]'$ denotes the metallicity if the efficiency of the star burst is reduced from 99 to 50 per cent. The burst epoch at 8 Gyr is chosen.

global	burst	$[\text{Mg}/\text{Fe}]$	$[\text{Fe}/\text{H}]$	$[\text{Fe}/\text{H}]'$
1.0	0.0	0.04	0.00	0.00
0.9	0.1	0.06	0.10	0.05
0.7	0.3	0.11	0.30	0.18
0.5	0.5	0.15	0.44	0.29
0.3	0.7	0.18	0.54	0.37
0.1	0.9	0.21	0.63	0.45
0.0	1.0	0.23	0.66	0.50

of the burst population if a shallow IMF ($x = 0.8$) during the burst is assumed. The chemical evolution of the global ISM is based on Salpeter IMF ($x = 1.35$) as before. It turns out that, with a significant flattening of the IMF, the major merger burst produces a metal-rich α -enhanced stellar population. As demonstrated in the left-hand panel of Fig. 3, the bulk of ellipticals experience their major merger at look-back times of 7–9 Gyr ($z \approx 0.7–1.5$) and therefore exhibit significant α -enhancement in the burst population.

5 GLOBAL–BURST MIXTURES

The question is how do the global and the burst populations mix? The value $x = 0.8$ represents the minimum flattening required for the case that the pure burst population is observed, i.e. in the centre of the galaxy. Apart from the fact that no mixing of the two population types seems unlikely, it would produce metallicity gradients much too steep. Table 1 gives the average abundance ratios for different mixtures of the global (IMF slope $x = 1.35$) and the 8 Gyr-burst populations ($x = 0.8$). $[\text{Fe}/\text{H}]'$ denotes the metallicity if the efficiency of the star burst is reduced from 99 to 50 per cent. Mg/Fe is not significantly affected (Thomas et al. 1999).

If the burst population mixes homogeneously with the

Table 2. Abundance ratios in the three zones separated by r_i and r_e . The first column gives the fraction of total light provided by the respective zone, cols. 2 and 3 specify the global-burst mixtures within each zone. $[\text{Fe}/\text{H}]'$ is explained in the caption of Table 1.

zone	light	global	burst	$[\text{Mg}/\text{Fe}]$	$[\text{Fe}/\text{H}]'$
$0 < r < r_i$	0.05	0.1	0.9	0.21	0.45
$r_i < r < r_e$	0.45	0.5	0.5	0.15	0.29
$r_e < r < \infty$	0.50	0.9	0.1	0.06	0.05

global population by providing 30 per cent of the total V -light, the resulting $[\text{Mg}/\text{Fe}]$ is reduced to 0.11 dex (row 3 in Table 1). For such proportions, the extreme flattening of $x = 0$ would be required to obtain a significantly α -enhanced population of $[\text{Mg}/\text{Fe}] = 0.2$ dex. More likely, however, is that the burst populations are more prominent in the inner parts due to dissipation processes in the burst gas (Barnes & Hernquist 1996). Table 1 can then be interpreted in terms of increasing galaxy radius from bottom to top. Abundance gradients result according to the global-burst mixtures assumed at different radii of the object.

I shall briefly discuss the following model, in which I roughly divide the galaxy in three zones separated by the inner radius r_i and the effective radius r_e . The resulting stellar abundance ratios in each zone for the respective different global-burst mixtures are shown in Table 2. Column 2 gives the V -light fraction of each zone, namely 5 per cent from the most inner part, and half of the light within the effective radius r_e . Altogether, the fractional contributions are chosen such that the burst population contributes 30 per cent of the total V -light of the galaxy. The star formation efficiency of the burst population is assumed to be 50 per cent, in order to avoid metallicities that exceed observational determinations. In Table 2, the quota of the burst population is steadily decreasing towards the outer zones of the galaxy, which leads to gradients such that both Mg/Fe and Fe/H are decreasing with increasing radius.

The galaxy nucleus is most metal-rich and significantly α -enhanced, the gradients of both Mg/Fe and Fe/H within r_e , however, are rather shallow. Thus this model predicts

the Mg/Fe overabundance not to decline remarkably out to r_e , in accordance with Worthey et al. (1992) and Davies et al. (1993). It is interesting to mention that the tendency of a slight decrease in α -enhancement is found in the Coma cluster sample analysed by Mehlert et al. (in preparation). The gradient in metallicity as given in Table 2 is also consistent with estimates by Davies et al. (1993) and Kuntschner (1998).

Finally it should be emphasized, that reasonable metallicities are only achieved if star formation during the burst is assumed to be efficient by only 50 per cent. Table 1 shows that otherwise metallicities above $3 Z_{\odot}$ would be obtained in the centre, which exceeds observational determinations (Kuntschner & Davies 1998).

6 DISCUSSION

It should again be emphasized that the SFHs discussed here are averages over many Monte Carlo realizations, individual galaxies are therefore not considered. This approach is sensible because also the observational constraint is taken to be a mean α -enhancement about which the values measured for the single galaxies scatter. Still, in a more detailed analysis it would be of great interest to resolve the SFHs of individual galaxies and to compare the theoretical scatter in α -enhancement with the observed one.

In the following I will discuss uncertainties in chemical evolution that may have an important impact on the results. Furthermore possible implications on properties of cluster and field galaxies are mentioned.

6.1 SN Ia rate and stellar yields

The model of chemical evolution applied for this analysis is calibrated such that the basic local abundance features are covered (Thomas et al. 1998). Besides stellar yields and IMF, this also includes the prescription of the Type Ia supernova, which is adopted from Greggio & Renzini (1983). According to this model, the maximum of the SN Ia rate occurs roughly 1 Gyr after the birth of the stellar population. It is obvious that this time-scale has a great impact on the results presented here. From the solar neighbourhood data, one cannot entirely exclude a SN Ia rate which sets in later and stronger. Such a model would basically delay (not prevent) the decrease of the Mg/Fe ratio, hence in the hierarchical clustering scheme the *global* populations of ellipticals would still not appear α -enhanced. However, the Mg/Fe ratios in the ISM would be higher *at the major burst epochs*, leading to more α -enhancement in the burst populations.

Uncertainties in stellar yields (Thomas et al. 1998) allow to raise the calculated Mg/Fe ratios. Note, however, that the degree of α -enhancement used as the main constraint in this paper ($[\alpha/\text{Fe}] = 0.2$ dex) represents the lowest limit determined from observational data.

A very early chemical pre-enrichment by PopIII-like objects may induce initial conditions in favour of high Mg/Fe ratios. The results in this paper, however, are not seriously affected by such uncertainties, since it is argued differentially to the solar neighbourhood chemistry on which the chemical evolution model is calibrated. Thus details of the

overall chemical initial conditions in the early universe do not alter the conclusions.

6.2 Selective mass loss

Type Ia supernovae explode later than Type II, thus their ejection occurs at different dynamical stages of the merging history. In a scenario in which Type Ia products (basically iron) are lost easier, the accomplishment of enhanced Mg/Fe ratios is simplified. The examination of this alternative, however, requires a more detailed analysis of the possible outflow and star formation processes during the merging history, which by far exceeds the scope of this paper. On the other hand it is important to notice, that α -enhanced giant elliptical galaxies enrich – for Salpeter IMF – the intra-cluster medium (ICM) with Mg/Fe *underabundant* material (Thomas 1998b). A selective loss mechanism as mentioned above further increases this ICM-galaxy asymmetry (Renzini et al. 1993) and therefore causes a more striking disagreement with observational measurements which indicate solar α/Fe ratios in the ICM (Mushotzky et al. 1996; Ishimaru & Arimoto 1997).

6.3 Cluster vs. Field

The SFH discussed in this paper applies to *cluster* ellipticals. In such a high density environment, the collapse of density peaks on galaxy scale is boosted to high redshifts (K96). In the low-density surroundings of the field (haloes of $10^{13} M_{\odot}$), instead, the situation is entirely different. The K96 model predicts that objects in the field are not destined to be ellipticals *or* spirals, but actually undergo transformations between both types due to gas accretion (formation of a disc galaxy) or merging of similar sized spirals (formation of an elliptical). As a consequence, the objects we happen to observe as bright ellipticals in the field should have mostly had a recent merger in the past 1.5 Gyr. This leads to younger mean ages, but also to a more extended SFH. Figs. 1 and 3 show that later bursts yield lower Mg/Fe ratios. From the models, one should therefore expect a trend such that (bright) ellipticals in the field are on average *less* α -enhanced than their counterparts in clusters (see also Thomas 1998a). Thus, the *intrinsic* difference between cluster and field ellipticals (K96), which manifests itself most prominent in the properties of *bright* elliptical galaxies, should be measurable in their α -element abundance patterns.

7 CONCLUSION

In this paper, I analyse average star formation histories (SFH) as they emerge from hierarchical clustering theory with respect to their capability of producing α -enhanced abundance ratios observed in elliptical galaxies. For this purpose, the V -luminosity weighted age distributions for the stellar populations of the model spiral and cluster elliptical galaxy are adopted from Kauffmann (1996, K96).

Owing to the constant level of star formation in spiral galaxies, their SFH leads to roughly solar Mg/Fe ratios in the stars *and* in the ISM, in agreement with observations in the Milky way. For elliptical galaxies, hierarchical models predict more star formation at high redshift and therefore

significantly older mean ages. However, the calculations in this paper show, that their SFH is still too extended in order to accomplish a significant degree of *global* α -enhancement in the stars. Star bursts ignited by the major merger when the elliptical forms, instead, provide a promising way to produce metal-rich Mg/Fe overabundant populations, under the following assumptions:

- (i) The nucleus predominantly consists of the burst population formed in the major merger.
- (ii) The burst population provides roughly 30 per cent of the total V -light of the galaxy.
- (iii) The IMF is significantly flattened ($x \lesssim 0.8$) *during the burst* with respect to the Salpeter value ($x = 1.35$).
- (iv) The efficiency of star formation during the burst has to be reduced to roughly 50 per cent, in order to guarantee shallow metallicity gradients within the galaxy.

The burst populations and its proportions to the global populations turn out to occupy a crucial role in producing Mg/Fe overabundance in the framework of hierarchical galaxy formation.

A direct consequence of the model is a slight gradient in α -enhancement in terms of decreasing α/Fe with increasing radius. A further implication is that bright *field* ellipticals are predicted to exhibit lower α/Fe ratios than their *cluster* counterparts, due to the younger mean ages and hence more extended SFHs of the former. A future theoretical task will be to directly combine the chemical evolution of α -elements and iron with semi-analytic models in order to allow for a more quantitative analysis than provided by this paper.

ACKNOWLEDGMENTS

I am very grateful to R. Bender and L. Greggio, who provided the mental foundation stones of this work and gave important comments on the manuscript. G. Kauffmann, the referee of the paper, is particularly acknowledged for very important suggestions that significantly improved the first version. I also thank C. Baugh, J. Beuing, S. Cole, N. Drory, H. Kuntschner, C. Lacey, C. Maraston, D. Mehlert and R. Saglia for interesting and helpful discussions. This work was supported by the "Sonderforschungsbereich 375-95 für Astro-Teilchenphysik" of the Deutsche Forschungsgemeinschaft.

REFERENCES

Arimoto N., Yoshii Y., 1987, *A&A*, 173, 23
 Barnes J. E., Hernquist L., 1996, *ApJ*, 471, 115
 Baugh C. M., Cole S., Frenk C. S., 1996, *MNRAS*, 283, 1361
 Bender R., 1997, in Arnaboldi M., Da Costa G. S., Saha P., ed, *The second Stromlo Symposium: The nature of elliptical galaxies*. Brigham Young University, Provo, p. 11
 Bender R., Burstein D., Faber S. M., 1993, *ApJ*, 411, 153
 Bower R. G., Lucey J. R., Ellis R. S., 1992, *MNRAS*, 254, 589
 Bower R., Kodama T., Terlevich A., 1998, *MNRAS*, 299, 1193
 Cole S., Aragón-Salamanca A., Frenk C. S., Navarro J., Zepf S., 1994, *MNRAS*, 271, 781
 Davies R. L., Sadler E. M., Peletier R. F., 1993, *MNRAS*, 262, 650
 Gould A., Bahcall J. N., Flynn C., 1997, *ApJ*, 482, 913
 Greggio L., Renzini A., 1983, *A&A*, 118, 217

Ishimaru Y., Arimoto N., 1997, *PASJ*, 49, 1
 Jimenez R., Friça A. C. S., Dunlop J. S., Terlevich R. J., Peacock J. A., Nolan L. A., 1999, *MNRAS*, submitted, astro-ph/9812222
 Jørgensen I., Franx M., Kjaergaard P., 1996, *MNRAS*, 280, 167
 Kauffmann G., 1996, *MNRAS*, 281, 487
 Kauffmann G., Charlot S., 1998, *MNRAS*, 294, 705
 Kauffmann G., White S. D. M., Guiderdoni B., 1993, *MNRAS*, 264, 201
 Kauffmann G., Charlot S., White S. D. M., 1996, *MNRAS*, 283, L117
 Kuntschner H., 1998, Phd thesis, University of Durham, Durham
 Kuntschner H., Davies R. L., 1998, *MNRAS*, 295L, 29
 Lacey C. G., Guiderdoni B., Rocca-Volmerange B., Silk J., 1993, *ApJ*, 402, 15
 Matteucci F., 1994, *A&A*, 288, 57
 Mushotzky R., Loewenstein M., Arnaud K. A., Tamura T., Fukazawa Y., Matsushita K., Kikuchi K., Hatsukade I., 1996, *ApJ*, 466, 686
 Nomoto K., Hashimoto M., Tsujimoto F.-K., Kishimoto N., Kubo Y., Nakasato N., 1997, *Nucl. Phys. A*, 616, 79c
 Peletier R., 1989, Phd thesis, Rijksuniversiteit Groningen
 Renzini A., Ciotti L., D'Ercole A., Pellegrini S., 1993, *ApJ*, 419, 52
 Salpeter E. E., 1955, *ApJ*, 121, 161
 Thielemann F.-K., Nomoto K., Hashimoto M., 1996, *ApJ*, 460, 408
 Thomas D., 1998a, in Carral P., Cepa J., ed, *Star Formation in Early-Type Galaxies*. ASP Conf. Ser., astro-ph/9808262
 Thomas D., 1998b, in *Chemical Evolution from Zero to High Redshift*. Springer, ESO workshop, astro-ph/9811409
 Thomas D., Greggio L., Bender R., 1998, *MNRAS*, 296, 119
 Thomas D., Greggio L., Bender R., 1999, *MNRAS*, 302, 537
 Tinsley B. M., 1980, *Fundam. Cosmic Phys.*, 5, 287
 Woosley S. E., Weaver T. A., 1995, *ApJS*, 101, 181
 Worthey G., 1994, *ApJS*, 95, 107
 Worthey G., Faber S. M., González J. J., 1992, *ApJ*, 398, 69